DYNAMIC EVOLUTION OF CORONAL MAGNETIC FIELDS

Richard S. Steinolfson
Institute for Fusion Studies
University of Texas at Austin
Austin, Texas 78712

ABSTRACT

The response of coronal magnetic fields to photospheric motion is investigated using a time-dependent, two-dimensional MHD simulation. Starting with an initially uniform field, a circular section of the loop base is slowly rotated to represent the photospheric motion. The field lines at the base move with this flow in a manner consistent with the generated electric fields. The subsequent evolution of the field and flow can be characterized as passing through several distinct configurations. In the earliest phase the kinetic energy is negligible, and the current and field are parallel throughout most of the cylinder. This is followed by a period in which the field rotation increases, the axial field at and near the axis increases, and the axial field decreases in two cylindrical regions away from the axis. When the field in an appreciable portion of the cylinder has undergone one complete rotation, a rapid change in field configuration occurs with a large portion of the field making several rotations at large radii and a corresponding large reduction in the axial field.

INTRODUCTION

Based on the assumption that the energy source for some of the explosive behavior observed in the solar corona (e.g., flares, eruptive prominences) is the in-situ magnetic field, there has been considerable interest over the years to develop theories and, more recently, numerical models to describe the generation of this nonpotential magnetic energy. The present study will be concerned with the coronal loop, in which compact flares may occur, as opposed to coronal arcades, in which eruptive prominences and the more energetic two-ribbon flares may originate.

In the case of loops, one theory advocates their emergence from the convective zone as highly concentrated helically twisted flux ropes (Piddington, 1975). The problem here is to explain how the loop remains stable for relatively long time periods before suddenly going unstable. In this study, we adopt the opposing view that sheared, twisted fields in coronal loops form as a result of convective or photospheric motion at the base of initially potential coronal magnetic configurations.

Numerous studies of magnetic energy build-up in coronal fields have been based on the premise that the field evolution must satisfy the requirement of a vanishing Lorentz force (e.g., Sturrock and Woodbury, 1967; Zweibel and Boozer, 1985). The reasoning here being that unrealistically large thermal pressures would be required to balance the Lorentz force in the relatively low beta corona: a not unreasonable argument **providing** the dynamics are neglected. However, when the coronal motion is included in a low beta (ratio of thermal to magnetic pressures) plasma, a simple order-of-magnitude analysis estimates the following relation between the changes in velocity and magnetic field ($\delta v, \delta B$), the instantaneous values (v, B) and the local Alfven velocity (v_a) when $\mathbf{J} \times \mathbf{B} \neq 0$:

$$\frac{v}{v_a^2}\delta v \approx \frac{\delta B}{B}.$$

Hence, as would be expected, the unbalanced Lorentz force can be balanced by the flow dynamics, although the question remains as to how large these flows must be. We now explore the interaction between the field and flow. For the simulation presented herein, the Lorentz force in the latter stages of evolution is far from vanishing, and the nonpotential magnetic energy is considerably larger than the kinetic energy.

MODEL AND COMPUTATIONAL PROCEDURE

A coronal loop is approximated by a cylinder with an initially uniform magnetic field. For this exploratory study gravity is neglected, the evolution is axisymmetric, and the corona is treated as

incompressible with a low enough beta that thermal pressure gradients are negligible. The dynamics now uncouple from the energetics, and the equations that must be solved are the following:

$$\frac{d\vec{v}}{dt} = \frac{1}{4\pi\rho}(\nabla \times \vec{B}) \times \vec{B},$$

$$\frac{\partial \vec{B}}{\partial t} = \nabla \times \left(\vec{v} \times \vec{B} - \frac{c^2\eta}{4\pi}\nabla \times \vec{B}\right).$$

These equations are solved numerically using the semi-implicit method of Harned and Kerner (1985). This differencing scheme offers the advantage of permitting time steps larger than those imposed by the fast modes (the explicit CFL condition). In addition, it is relatively simple to code, and the computing time for each time step is comparable to that for explicit methods. An extension of this method by Harned and Schnack (1986), which removes the shear Alfven constraint and thereby remains stable for even larger time steps, is currently being investigated.

The boundary conditions at the loop center are trivial in this axisymmetric simulation. The maximum radius of the computational cylinder is large enough (twice the radius within which the base is rotated) that the physicial variables at this boundary are not modified significantly: zero-order extrapolation is sufficient. At the loop mid-point a form of symmetry conditions, consistent with each end of the loop being rotated by the same amount in opposite directions, is used. The only velocity at the base is the rotation (azimuthal) velocity, which increases linearly out to three-fourths the maximum rotation radius and then decreases linearly to zero. The azimuthal magnetic field at the base is updated at each time step using the ideal induction equation, and zero-order extrapolation provides the radial field. The axial field is maintained constant at its initial uniform value at the base in order that the flux into the loop remain constant. One check on the numerical solution is to compute the flux through the loop mid-point. For the simulation in the following section, this flux remained within a few percent of the flux into the loop.

NUMERICAL RESULTS

The physical conditions for the simulation discussed here are: density = 10^9 cm^{-3}, initial magnetic field = 10.54g, temperature= 1.6×10^6 K, Lundquist number = 10^4, maximum rotation radius (a, the value used to normalize distance) = 10^9 cm, total loop length = 2×10^9 cm. The initial beta and Alfven velocity then become 0.1 and 727 km s^{-1}. The maximum rotation velocity is 10 km s^{-1}, which is 1.4% of the initial Alfven velocity.

The evolution of the magnetic and kinetic energies is shown in Fig. 1. The plotted value is the nonpotential magnetic energy or that in excess of the initial value of 5.5×10^{28} ergs. As illustrated in the figure, the current and field are approximately parallel in the early stages when the kinetic energy is negligible relative to the excess magnetic energy. This is true throughout the cylinder with the exception of thin layers at the cylinder base and center. Although the current and field are parallel (i.e., $\mathbf{J} = \alpha\mathbf{B}$), the quantity α varies considerably in space (for t = 19.4 min., $-6 < \alpha < 1.5$).

After approximately twenty minutes, the kinetic energy rises rapidly followed by a period of slower growth when both energies grow exponentially at about the same rate. After this latter stage both energies increase dramatically. The magnetic configuration differs in the above three phases (negligible kinetic energy, uniform growth, rapid rise), and each of these is discussed below.

The approximate exponential growth of the magnetic energy (up to the last phase) occurs at a rate of 0.036 in terms of the initial Alfven time. (For comparison, this is about equal to the maximum growth of the tearing mode at a Lundquist number of 10^3.) The present growth rate is independent of the Lundquist number.

Some of the field lines, typical of the field evolution in the first phase (negligible kinetic energy), are shown in Fig. 2. Distances in this and subsequent figures are normalized to the maximum rotation radius at the base, and the circle indicates the location of the maximum rotation. The azimuthal component has been zeroed out for this presentation to illustrate how these results compare with the analytic solution of Zweibel and Boozer (1985; Fig. 1). Both solutions indicate a bending of the field line

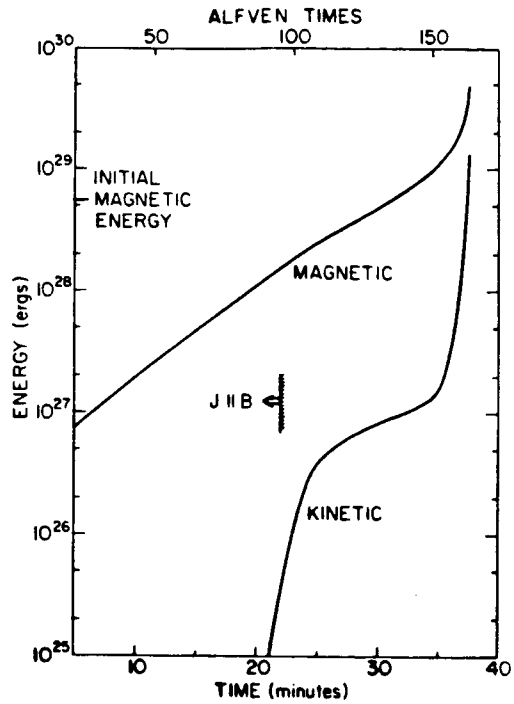

Figure 1. Temporal increase in excess magnetic and kinetic energies integrated over one half the cylinder length.

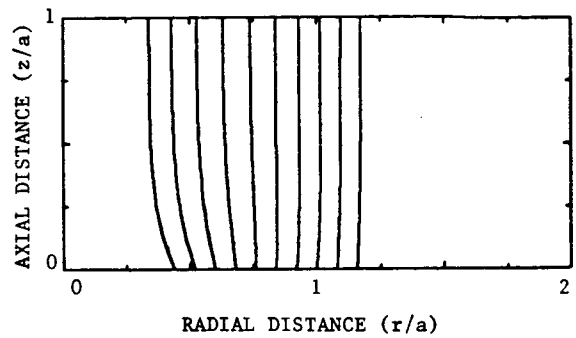

Figure 2. Field lines projected into the r-z plane for t = 19.4 minutes.

toward the axis (which is largest near the base) inside the maximum twist location, and a slight outward bending beyond the twisted region. Between the base and the loop mid-point, the field lines are rotated by a maximum of about 70° for the solution in Fig. 2. The increase in the axial field strength near the cylinder axis (and the consequent inward bending of the field lines) coincides with an azimuthal current in the positive azimuthal direction that peaks at a radius of about 0.2.

The primary current system established in the first phase prevails during the subsequent evolution. This system consists of (a) an axial current concentrated near the axis flowing toward the base, (b) a radial current inside the maximum rotation radius near the base and directed away from the axis, and (c) the azimuthal current referred to above. In the later stage additional currents develop near the radius of maximum twist and beyond.

During the second phase when the magnetic and kinetic energies grow at similar rates, the field twist and shear continually increase. The field lines near the transition between the second and third phase are shown in several views in Fig. 3. Notice that two field lines now undergo approximately one complete rotation between the base and loop mid-point. One starts at the base at the location of maximum rotation and the other is at the edge of the rotated region. It is interesting that the lines between these two only rotate about half as much. This behavior is mainly due to the fact that the lines with the large twist pass through regions where the axial field strength has been reduced to about 10% of its initial value, while between these regions the axial field increases by about 10%. Azimuthal currents in the negative (positive) azimuthal direction just inside (outside) the maximum rotation and the primary currents near the axis are consistent with the modified axial field. An axial current centered at maximum rotation flowing away from the base contributes to the large rotation at large radii.

A dramatic change in the field configuration occurs in the short interval (~ 18 sec) between the times in Fig. 3 and Fig. 4. Notice that this reconfiguration only occurs for the field lines originating at the location of maximum twist and beyond. The inner four field lines remain virtually unaffected. The axial field strength is now reduced substantially (down to 1% of the initial value) in a large region ($0.75 < r < 1.5$ and $0.2 < z \leq 1$). This axial field reduction permits some field lines to rotate several times before reaching the loop mid-point, as seen in Fig. 4 (a), (b). (Numerical problems are responsible for not

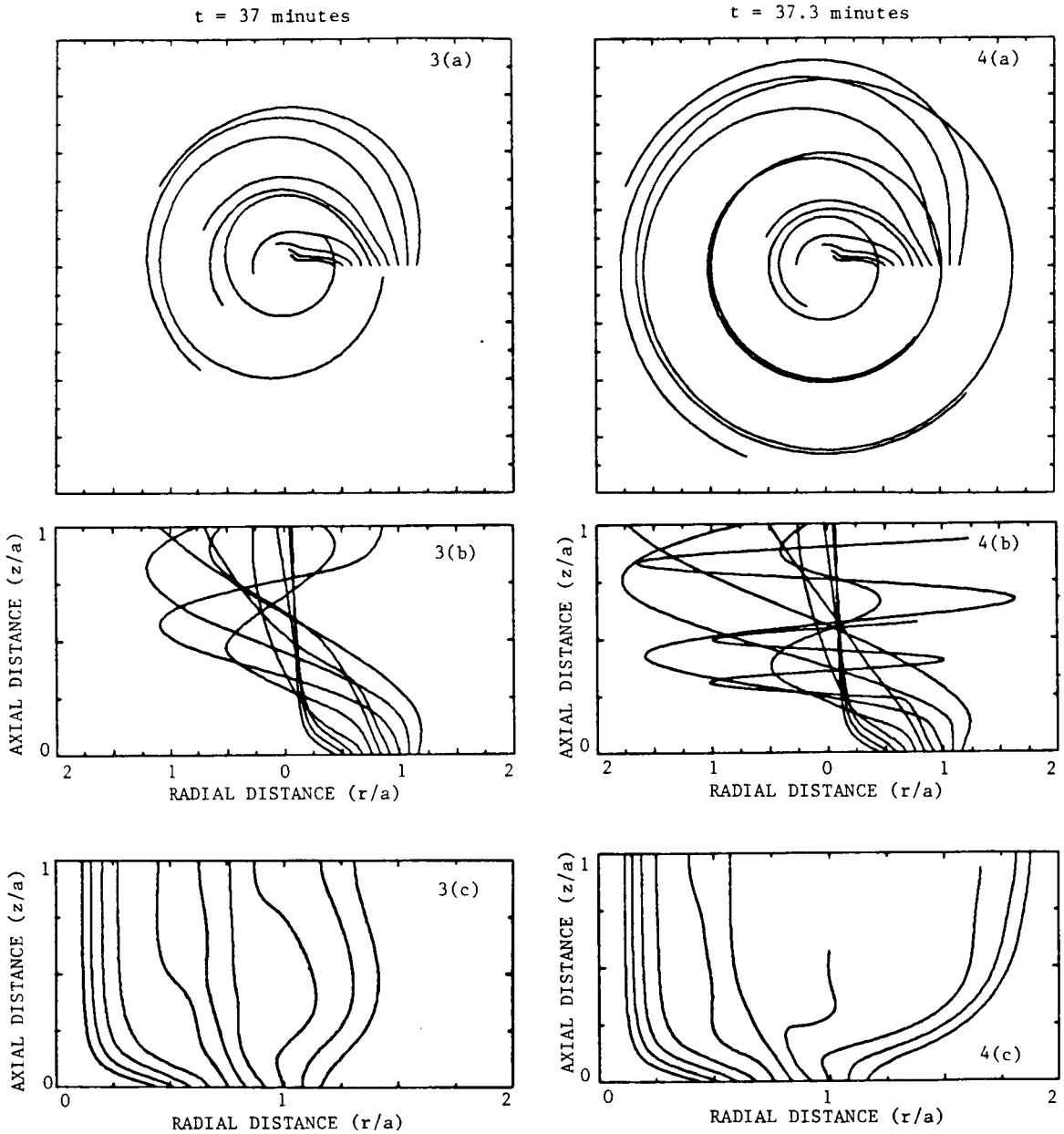

Figures 3,4. Field lines near the end of the uniform growth (37 minutes) and in the rapid growth (37.2 minutes) phase. The same field lines are shown in all views at both times. The field lines as they would appear when seen from the cylinder base are drawn in the top figures (a), and the view from the side is shown in the center figures (b). The bottom figures (c) correspond to the projection in Figure 2. The field line with the circle at the base is at the location of maximum rotation.

extending the two field lines to the mid-point in Fig. 4(b), (c)).

The axial field does not appear to have reversed direction in this simulation, although it does become very small. (Note that the fields may have temporarily reversed at times that were not selected for display.) In other simulations where the rotation velocity is a larger fraction of the initial Alfven velocity (a higher density was used with the same rotation velocity), the axial field does reverse, and magnetic islands are formed for relatively short time periods. The qualitative evolution of this latter computation, however, is the same as for the solution discussed here.

Another reconfiguration occurs 0.2 minutes after the time used for the results in Fig. 4. In this case all of the field lines shown in Figs. 2-4 collaspe toward the axis with comparatively small rotation (less than 270 degrees) and with the same general shape as the inner four lines in Fig. 3(c) and Fig. 4(c). This stage is not discussed further since it is questionable whether such behavior would ever be obtained if the solution had the extra degree of freedom available in a three-dimensional simulation.

CONCLUSION

This study has shown that photospheric motion can produce enough free magnetic energy in an initially potential magnetic loop to explain the energy source of the compact flare. However, in contrast to assumptions that are frequently made, the energy build-up does not evolve through a series of equilibrium states, the current and field do not remain parallel during the process, and when the current and field are parallel the proportionality between them (α) varies in space.

ACKNOWLEDGMENTS

The author has benefited considerably from conversations with Drs. D. Barnes, Z. Mikic, D. Schnack, T. Tajima, and E. Zweibel. This work was initiated with support from AFGL contract F19628-85-K-0006 and currently receives support from NASA under grant NAGW-846 and from the Atmospheric Science Section of NSF under grant ATM 85-06646. Acknowledgment is also made to NSF for providing computer time at the San Diego Supercomputer Center.

REFERENCES

Harned, D.S., and Kerner, W. 1985, *J. Comp. Phys.*, **60**, 62.

Harned, D.S., and Schnack, D.D. 1986, *J. Comp. Phys.* (in press)

Piddington, J.H., 1975, *Astrophys. Space Sci.*, **34**, 347.

Sturrock, P.A., and Woodbury, E.T. 1967, **Plasma Astrophysics**, ed. P.A. Sturrock (New York: Academic), p. 155.

Zweibel, E.G., and Boozer, A.H. 1985, *Ap. J.*, **295**, 642.